Forced Entanglement vs Anisotropic Dissipation in a Vortex Line Liquid

D. López,[1] L. Krusin-Elbaum,[1] H. Safar,[2] V. M. Vinokur,[3] A. D. Marwick,[1] J. Z. Sun,[1] and C. Feild[1]
[1]*IBM Research, Yorktown Heights, New York 10598*
[2]*Department of Physics, University of Illinois at Chicago, Chicago, Illinois 60607*
[3]*Argonne National Laboratory, Argonne, Illinois 60439*
(Received 5 May 1997)

We present evidence for *forced topological entanglement* of line-like vortices in the liquid regime of $YBa_2Cu_3O_{7-\delta}$ with columnar defects. By splaying the defects within a fixed plane (in-fan) we create a $\hat{\mathbf{c}}$-axis phase coherent vortex (string) structure which correlates with anisotropic dissipation. The high-field vortex motion is "easy" in fan and "hard" across fan in crystals—a signature of forced entanglement by a small angle splay. The high-field anisotropy is surprisingly reversed in thin films, where forced entanglement is absent. [S0031-9007(97)04606-1]

PACS numbers: 74.60.Ge, 74.72.Bk

The idea of entangled vortex matter [1] in type II superconductors is central to understanding the behavior of a vortex liquid [2] and possibly a disordered vortex solid [3]. There are two kinds of entanglement. Thermal entanglement is connected to *melting* of the vortex array. Current debate centers on melting accompanied by a loss of the transverse [4] and, less trivially, of the $\hat{\mathbf{c}}$-axis long range superconducting coherence [5]. The latter manifests itself as a loss of *vortex coherence*, i.e., a loss of the identity of individual vortex lines, which split into *decoupled* segments of finite length. Recent reports suggest that twin boundaries [5] or technologically important columnar defects [6,7] *recouple* vortex segments and maintain the line-like structure of vortices far into the liquid regime [8]. On the other hand, as discussed in theory by Hwa *et al.* [9], the localizing action of columnar pins [10] can be used to force *topological vortex entanglement* by manipulating (splaying) the defect configurations [11]. Such *forced* entanglement occurs only with line-like vortices, for which the *vortex coherence* is preserved. Thus, splayed columnar pins provide a unique controllable tool to probe the $\hat{\mathbf{c}}$-axis coherence in the entire mixed state.

In this Letter, we explore the consequences of the $\hat{\mathbf{c}}$-axis coherence to the dissipation in the vortex liquid. We present evidence for forced topological entanglement of line-like vortices in $YBa_2Cu_3O_{7-\delta}$ (YBCO) with the simplest *splayed* columnar defect configuration [9], namely, two parallel pin families crossing each other in a (splay) plane at a fixed angle Θ [see inset in Fig. 1(a)]. Our key result is that in crystals with not too large Θ [11], the vortex motion is "easy" parallel to the plane of splay (SP) and "hard" across this plane everywhere where the *linear* resistance ($R_{\rm lin} = \lim_{I\to 0} \frac{V}{I}$) [12] along the field ($\hat{\mathbf{c}}$-)direction vanishes, indicating a presence of coherent vortex lines across the sample. Anisotropy disappears when the splay angles are either large or zero (parallel defects)—the former is in accordance with our expectations that for large Θ the $\hat{\mathbf{c}}$-axis coherence cannot be maintained, since vortex cutting becomes easy [13]. The latter ensures that anisotropy is indeed related to the effect of splay. Moreover, the anisotropy disappears at low magnetic fields (below a fraction of the matching field B_Φ, at which the number of vortices equals the number of pins [7]), indicating a change in the character of pinning related to occupation of columnar tracks. In thin films, in the absence of entanglement, the observed *high-field anisotropy is reversed* (i.e., the motion across fan becomes favored), while the dissipation below $\sim 0.5B_\Phi$ is still isotropic.

Several twinned YBCO crystals of $\sim$1 mm size and 11 to 15 μm thick along the $\hat{\mathbf{c}}$ axis [11] and $\hat{\mathbf{c}}$-axis oriented epitaxial films grown by laser ablation [14] were irradiated with 1.08 GeV $^{197}Au^{23+}$ at the TASCC facility at Chalk River Laboratories in Canada [7]. To install planar splay, the ion beam was tilted off the $\hat{\mathbf{c}}(\hat{z})$ axis by rocking the samples about an axis $\perp\hat{z}$ by $\pm\Theta$ ranging from 0° to 45° [a cross-sectional transmission electron micrograph (TEM) of crossing tracks [11] is an inset of Fig. 1]. The films were patterned (on the same chip) prior to irradiation in a bridge geometry, allowing control of the relative orientation between the driving current and splay planes. Resistivities were measured using a standard four-probe technique. In crystals the contacts pads were placed as to assure a uniform current flow [5].

Figure 1(a) shows the temperature variation of the in-plane dissipation for $\mathbf{H} \parallel \hat{\mathbf{c}}$ of a twinned $\simeq$12 μm thick YBCO crystal with a planar splay configuration with a criss-cross angle $\Theta = \pm 10°$ and a total pin density corresponding to $B_\Phi = 3$ T. The vortices are forced to move either "across fan" [Lorentz force $\mathbf{F_L} = (\mathbf{J} \times \mathbf{B}) \perp$ SP] or "in fan" [$\mathbf{F_L} \parallel$ SP] in the *same* crystal by appropriately directing the measuring current. The zero-field resistive transition at $T_c \simeq 90$ K is independent of the current geometry—it is sharp ($\Delta T_c \approx 400$ mK), and only slightly ($\sim$1%) lower than in the same virgin sample. The data show that the two current geometries produce *isotropic* dissipation at low fields.

At high fields the *linear* (Ohmic) resistance is distinctly anisotropic below a characteristic temperature $T_a(H)$ [Fig. 1(a)]—*it is easier for the vortices to move parallel to the splay plane than across*, namely, $R_{ab}^{\perp} > R_{ab}^{\parallel}$. The

 0031-9007/97/79(21)/4258(4)$10.00

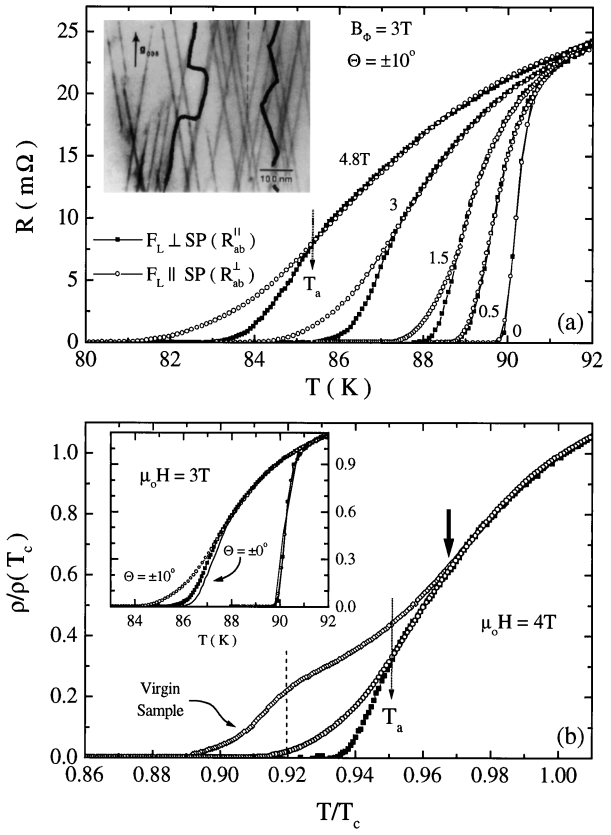

FIG. 1. Temperature dependences of the in-plane dissipation for $\mathbf{F_L} \perp$ SP (across fan) and $\mathbf{F_L} \parallel$ SP (in fan) in a twinned YBCO crystal with columnar tracks with density $B_\Phi = 3$ T and splay angle $\Theta = \pm 10°$ (a) in several fields $\parallel \hat{\mathbf{c}}$ axis and (b) in a 4 T field before and after irradiation with Au. Thick arrow points to the onset of pinning by columnar pins. Dotted arrows indicate the onset of anisotropy. Dashed line marks twin boundary shoulder at T_{TB}. The applied $I = 1$ mA. Top inset: cross-sectional TEM image of YBCO crystal thinned to $\leq$1000 Å, showing two families of parallel tracks criss-crossed at $\pm 10°$ in the splay plane. A double-kink and zigzag vortex excitations are sketched (see text). Bottom inset: comparison of the crystal of (a) with a similar crystal with $\parallel$ defects ($\Theta = 0$). Similar kink dynamics is suggested by a comparable dissipation for $\mathbf{F_L} \perp$ SP and for $\Theta = 0$ (see text).

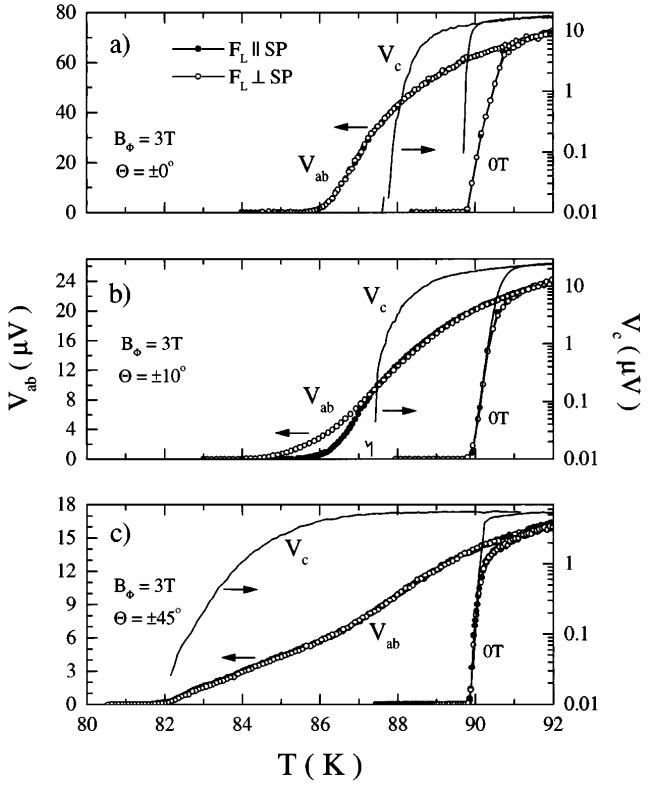

FIG. 2. Temperature dependences of the in-plane and $\hat{\mathbf{c}}$-axis Ohmic dissipation in YBCO crystals with (a) parallel pins, (b) $\pm 10°$ splay, and (c) $\pm 45°$ splay in a zero and 3 T applied field. The applied current is 1 mA.

resistance $R(T_a)$ at which the anisotropy becomes evident is field independent ($\sim 0.3 R_N$) and near the value at the shoulder in the resistance of the virgin crystal [Fig. 1(b)]. The shoulder at $T_{TB}(H)$, associated with the onset of twin boundary (TB) pinning [15], is well below $T_a(H)$—which leads us to conclude that the observed anisotropy is not due to twin boundaries [16]. The data also show that columnar tracks slow the vortex motion down (reduce R) well above the onset of anisotropic dissipation; linear resistivities for the virgin and irradiated crystal part at $\sim 0.97 T_c > T_a \sim 0.95 T_c$ [see Fig. 1(b)].

Now we ask what vortex structure might be associated with the anisotropic dissipation in the liquid. One measure of this structure is resistance along the field direction, which, if zero, will indicate vortex coherence on at least the scale of sample dimension [5]. Figure 2 contrasts the $\hat{\mathbf{c}}$ axis and the in-plane voltages for the two current geometries in three YBCO crystals with $B_\Phi = 3$ T: (a) with parallel pins, (b) with small ($\pm 10°$), and (c) large ($\pm 45°$) angle splay. For parallel pins ($\Theta = 0°$) the $\hat{\mathbf{c}}$-axis dissipation becomes non-Ohmic *above* the temperature where the *ab*-plane dissipation goes to zero. The in-plane motion here is isotropic as vortices move via double-kink spreading [10] for any current direction. This is illustrated in Fig. 2(a) for an ~ 11 μm thick crystal. A small splay ($\Theta = \pm 10°$) shifts the onset of coherence down—now the longitudinal voltage vanishes at $T_a(H)$ [see Fig. 2(b)], i.e., the onset of the $\hat{\mathbf{c}}$-axis phase coherence coincides with the onset of anisotropic vortex motion. In others words, only *line vortices* can distinguish between the two current geometries.

To test this further we examine a crystal of the same thickness (~ 11 μm) and B_Φ but with a much larger $\Theta = \pm 45°$. *Large angle splay will not support the* $\hat{\mathbf{c}}$*-axis coherence in the liquid* altogether as vortices will not easily accommodate to columnar pins [10] and the dynamics should be as with random point disorder. Data in Fig. 2(c) demonstrate that in this case all resistances vanish together; the response in the liquid along the $\hat{\mathbf{c}}$ (field) direction is *always linear*—thus there is no evidence for either a line liquid or anisotropy.

The anisotropy translates onto the H-T phase diagram as two distinct lines, shown in Fig. 3. At high fields, the

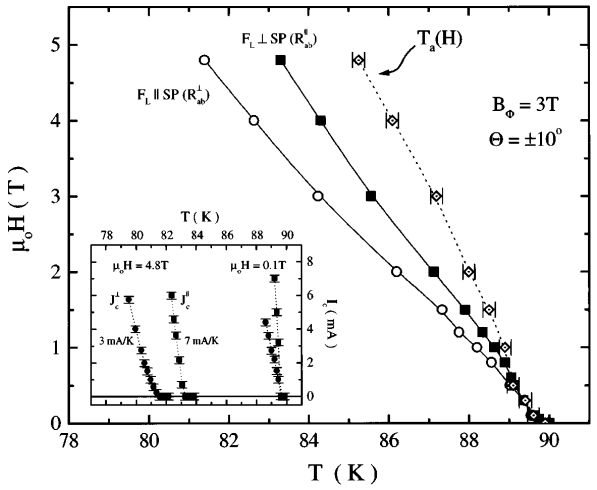

FIG. 3. *H-T* phase diagram for the YBCO crystal of Fig. 1. The two lines above a crossover at $\mu_0 H_{\rm cr} \sim 1$ T correspond to $R_{\rm lin} \to 0$ and the onset of nonlinear *I-V*'s for $\mathbf{F_L} \perp$ SP and $\mathbf{F_L} \parallel$ SP. The anisotropy in the in-plane resistance appears below $T_a(H)$, along which the coherence in the $\hat{\mathbf{c}}$-axis direction is restored. Inset: the in-plane critical currents maintain anisotropy at all fields.

in-plane linear resistivity $R^{\parallel}_{ab}$ for the across-fan motion vanishes at higher temperatures than $R^{\perp}_{ab}$ for the in-fan motion—the difference is quite large above B_Φ (2 K at $\mu_0 H \cong 5$ T), and it increases with field. The anisotropy disappears entirely below $\mu_0 H_{\rm cr} \sim 1$ T, where both in-plane resistivities as well as R_c *vanish simultaneously*. Above $B_{\rm cr}$ the lines for both current geometries look linear in reduced temperature $t = T/T_c$, while below they are upwardly curved, i.e., $\propto (1 - t)^\alpha$ with $\alpha \sim 2$ [17].

The vanishing of $R^{\perp}_{ab}$ and $R^{\parallel}_{ab}$ is followed by the appearance of critical currents $J_c^{\perp}$ and $J_c^{\parallel}$, shown in the inset of Fig. 3. J_c (obtained from the onset of nonlinearities in the *I-V* curves with the usual $\sim 1\ \mu$V/cm threshold) is anisotropic at *all* fields, namely, the hard direction $J_c^{\parallel}$ ($\mathbf{F_L} \perp$ SP) grows more than twice as fast with decreasing temperature as the easy direction $J_c^{\perp}$. In other words, unlike the anisotropy in the liquid phase, the J_c anisotropy (i.e., $dJ_c^{\parallel}/dT > dJ_c^{\perp}/dT$) is present also below the crossover at $B_{\rm cr}$. However, it appears that (within our resolution) above $B_{\rm cr}$ the two J_c's *vanish at different temperatures*, suggesting two transitions related to two distinct vortex structures at high fields [18]. Two different vortex structures are implicit in recent experiments and numerical simulations [11]. The motion across fan is primarily governed by spreading of the double kinks [9,10] [inset of Fig. 1(b)], while the in-fan motion will be controlled by the "zigzag" kinks [11] [inset of Fig. 1(a)], resulting in critical current anisotropy [19] with a reduced in-fan J_c.

The situation in the vortex liquid is more subtle and the above arguments cannot be simply projected onto the linear regime. The vortex motion is diffusive and vortex structure can only be maintained over a finite time t_{pl} [2]. Crudely speaking, large t_{pl} implies that vortices linger longer in the vicinity of the columnar tracks and can maintain the structure resembling the structure in the solid on this time scale. Experimental support for similar vortex structures in the liquid and in the solid comes from a very similar dissipation for $\mathbf{F_L} \perp$ SP and for the parallel pins with the same B_Φ [inset of Fig. 1(b)]—in both cases the dynamics in the solid regime is controlled by motion of the double kinks.

To gain insight into the splay induced anisotropy and the role of forced entanglement let us consider a correction $\delta\rho$ to the *linear* flux-flow resistivity $\rho \cong \rho_{ff}(1 + \delta\rho/\rho)$ due to splayed disorder following [2], p. 1252:

$$\frac{\delta\rho}{\rho} \sim \frac{\Delta}{a_0^2 \cos\Theta} \int_0^\infty dt \int d^2k [\cdots] k^2 e^{-k^2\langle u_T^2\rangle - Ck_x^2 t - t/t_{pl}}, \tag{1}$$

where the splay described by the factor $\exp(-Ck_x^2 t)$ is in $\hat{\mathbf{x}} - \hat{\mathbf{z}}$ plane and C is a combination of shear and tilt elastic moduli [20]. In Eq. (1) Δ is the disorder parameter [2], v is vortex velocity, and $\exp(-k^2\langle u_T^2\rangle)$ is the Debye-Waller factor resulting from thermal fluctuations of the vortex lines (u_T is the transverse thermal displacement). The factor $\exp(-t/t_{pl})$ accounts for a (viscous) state of the entangled liquid—forced entanglement will increase liquid viscosity and thus will increase t_{pl}. The term in the square bracket $[\cdots] = [(\sin k v t/v t)k]$ describes the in-fan motion when $k = k_x$ and across-fan (along $\hat{\mathbf{y}}$) motion when $k = k_y$. Thus, the anisotropy in this estimate is controlled by the relative importance of the vortex structure term $\exp(-t/t_{pl})$. If t_{pl} is very small, the contribution comes from small times t; term $-Ck_x^2 t$ can be neglected and the difference between $\hat{\mathbf{x}}$ and $\hat{\mathbf{y}}$ motion disappears. In the limit $t_{pl} \to \infty$, the integration of Eq. (1) leads to anisotropic motion with $\delta\rho^{\parallel} \sim \frac{1}{Cu_T^4}$ and $\delta\rho^{\perp} \sim \frac{1}{Cu_T^4}\frac{\sqrt{Ct_{pl}}}{u_T}$. The above estimate backs our two key observations: (i) the motion in the liquid is harder across fan than in fan, and (ii) the anisotropic motion requires entangled vortex lines retaining their identity (large t_{pl}).

Finally, we should not observe the effect of forced entanglement in thin ($\sim$1500 Å) YBCO films with thicknesses comparable to the entanglement length l_c [1]. A rough estimate gives $l_c \simeq a_0^2 \varepsilon_l / T \cong 2a_0$ near melting temperature T_m. Here, $\varepsilon_l = [\Phi_0/4\pi\lambda]^2$ is the line energy and $\lambda \sim 1400$ Å is the magnetic penetration length [2]. For our films, the estimate gives $l_c \cong 1000$ Å for $B \sim 1$ T. Furthermore, in contrast to crystals, in films with $B_\Phi = 5$ T the tracks rarely cross [21]. Thus in films a zigzag related anisotropy is not expected.

The results in films are summarized in the *H-T* diagram shown in Fig. 4. As before, at low fields the motion is isotropic. However, in contrast to crystals, the *high-field anisotropy above $B_{\rm cr}$ is reversed*, i.e., the in-fan motion is now hard. This is clearly seen in the inset, where we plot ρ vs temperature for $\mathbf{F_L} \perp$ SP and $\mathbf{F_L} \parallel$ SP on a log scale. A crossover at $B_{\rm cr} \sim 0.5 B_\Phi$ (as for the parallel pins [7]) is consistent with the absence of zigzagging.

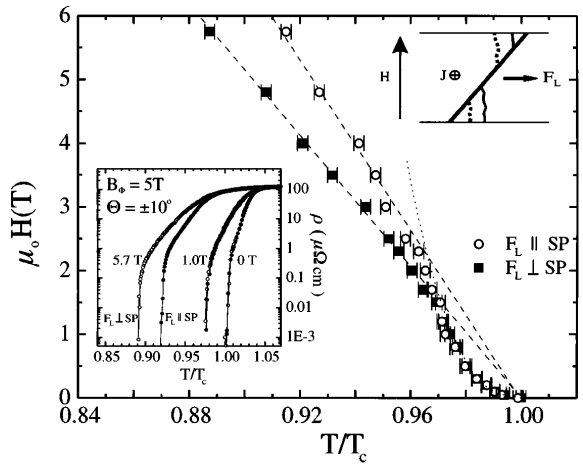

FIG. 4. H-T phase diagram for 1500-Å-thick epitaxial $\hat{\mathbf{c}}$-axis oriented YBCO films with a splay angle $\Theta \pm 10°$ and a total pin density $B_\Phi = 5$ T. The films were patterned as 8 μm wide transport bridges. The two lines above a crossover at $\mu_0 H_{cr} \sim 0.5 B_\Phi \cong 2.5$ T correspond to $R_{lin} \to 0$ for $\mathbf{F_L} \perp$ SP and $\mathbf{F_L} \parallel$ SP current geometries. The anisotropy in the in-plane resistances is reversed. Top inset: sketch of the relevant surface kinks for $\mathbf{F_L} \parallel$ SP. Bottom inset: the in-plane resistance vs temperature for $\mathbf{F_L} \perp$ SP and $\mathbf{F_L} \parallel$ SP for three values of applied field.

One clue to this surprising reverse anisotropy comes from realization that in films surfaces play a major role [22]. As vortices must satisfy the boundary conditions at the surfaces $\mathbf{S}$ ($\mathbf{B} \perp \mathbf{S}$), they will nucleate surface kinks on the length scale of λ at low fields, or on the length scale of a_0 (scaled by anisotropy [2]) when vortex-vortex interactions are relevant, and will spend only a small fraction of their length on columnar tracks in the film. A sketch in Fig. 4 illustrates how for $\mathbf{F_L} \parallel$ SP a trapped vortex segment will slide along the columnar track, so that the lagging (top) kink will shrink and the advancing (bottom) kink will expand. The top kink will be strongly pinned, since it is too costly to approach the surface at an angle Θ [23], and thus the in-fan motion can be more difficult than motion for $\mathbf{F_L} \perp$ SP which proceeds via energy-gaining *symmetric* expansion of surface kinks [2]. This surface-induced anisotropy in dynamics is not related to splay and should only depend on tilt of the pins with respect to the applied field [24].

In summary, we have demonstrated that in a splayed pinning landscape only a *coherent entangled* vortex structure can produce anisotropic dissipation in the liquid regime. The anisotropy sensitively depends on the rocking angle—for sufficiently small Θ vortex cutting is difficult and vortex lines can be forced to entangle. For sufficiently large ($\geq 45°$) Θ vortex cutting becomes easy and all the structure in the liquid is destroyed. Our results on recoupling provide support for the idea that melting is accompanied by the loss of $\hat{\mathbf{c}}$-axis coherence. A lack of anisotropy at low fields points to a deciding role of the occupancy of the columnar tracks even in the liquid phase.

We thank T. Hwa and L. Civale for stimulating discussions. The work at IBM was supported in part by EPRI Contract No. RP-8065-11 and by NSF GOALI Grant No. DMR-9510731. The work of V. M. V. was supported by the U.S. Department of Energy, BES-Material Sciences, under Contract No. W-31-109-ENG-38. We thank J. Hardy and J. Forster at TASCC-Chalk River, supported by AECL Research, for their help and the provision of irradiation facilities.

[1] D. R. Nelson, Phys. Rev. Lett. **60**, 1973 (1988).
[2] G. Blatter *et al.*, Rev. Mod. Phys. **66**, 1125 (1994).
[3] T. Giamarchi and P. LeDoussal, Phys. Rev. B **55**, 6577 (1997); J. Kierfeld, T. Nattermann, and T. Hwa, Phys. Rev. B **55**, 626 (1997); D. Ertas and D. R. Nelson, Physica (Amsterdam) **272C**, 79 (1996); M. Gingras and D. A. Huse, Phys. Rev. B **53**, 15 193 (1996).
[4] D. J. Bishop *et al.*, Science **255**, 165 (1992).
[5] D. López *et al.*, Phys. Rev. B **53**, R8895 (1996); Phys. Rev. Lett. **76**, 4034 (1996).
[6] L. Civale *et al.*, Phys. Rev. Lett. **67**, 648 (1991).
[7] L. Krusin-Elbaum *et al.*, Phys. Rev. Lett. **72**, 1914 (1994); Phys. Rev. B **53**, 11 744 (1996).
[8] E. F. Righi *et al.*, Phys. Rev. B **55**, 5663 (1997).
[9] T. Hwa *et al.*, Phys. Rev. Lett. **71**, 3545 (1993).
[10] D. R. Nelson and V. M. Vinokur, Phys. Rev. B **48**, 13 060 (1993).
[11] L. Krusin-Elbaum *et al.*, Phys. Rev. Lett. **76**, 2563 (1996).
[12] The nonlinear (current dependent) dissipation appears at the onset of finite J_c [2].
[13] N. K. Wilkin and M. A. Moore, Phys. Rev. B **47**, 957 (1993).
[14] J. Z. Sun *et al.*, Appl. Phys. Lett. **63**, 1561 (1993).
[15] W. Kwok *et al.*, Phys. Rev. Lett. **69**, 3370 (1992); S. Fleshler *et al.*, Phys. Rev. B **47**, 14 448 (1993).
[16] In *all* crystals in this study the angle current–twin boundary mosaic is $\sim 45°$.
[17] Such crossover is observed near half-filling $\sim 0.5 B_\Phi$ in the irreversibility lines of YBCO with parallel pins [7].
[18] We expect that the two transitions will merge with increasing sample thickness [5].
[19] Th. Schuster *et al.*, Phys. Rev. B **50**, 9499 (1994).
[20] $C = C_{66}\tilde{C}_{44}/(C_{66} + \tilde{C}_{44})$ contains splay modified tilt modulus $\tilde{C}_{44} = C_{44} tg^2\Theta$.
[21] The ab-plane view of the track shadows is that of short (~ 300 Å) lines in the splay plane with comparable separation in-plane and across given by the mean track distance $d = \sqrt{\Phi_0/B_\Phi} \sim 300$ Å.
[22] N. Schnerb, Phys. Rev. B **55**, 3382 (1997); Y. Simon *et al.*, Phys. Rev. B **50**, 3503 (1994).
[23] E. H. Brandt, Phys. Rev. B **48**, 6699 (1993).
[24] Experimentally, we find that YBCO films with parallel pins tilted off the $\hat{\mathbf{c}}$ axis by $\Theta = 10°$ show the same behavior as those with splay.